

See discussions, stats, and author profiles for this publication at: <https://www.researchgate.net/publication/258239412>

Ultralong CdTe Nanowires: Catalyst-Free Synthesis and High-Yield Transformation into Core-Shell Heterostructures

ARTICLE *in* ADVANCED FUNCTIONAL MATERIALS · JUNE 2012

Impact Factor: 11.81 · DOI: 10.1002/adfm.201102800

CITATIONS

14

READS

32

5 AUTHORS, INCLUDING:



[Yunchao Li](#)

Beijing Normal University

41 PUBLICATIONS 1,244 CITATIONS

[SEE PROFILE](#)

Ultralong CdTe Nanowires: Catalyst-Free Synthesis and High-Yield Transformation into Core–Shell Heterostructures

Feng Jiang, Jinjin Liu, Yunchao Li,* Louzhen Fan, Yuqin Ding, and Yongfang Li*

A novel catalyst-free synthetic strategy for producing high-quality CdTe nanowires in solution is proposed. A special reaction condition is intentionally constructed in the reaction system to induce the formation of nanowires through oriented *in situ* assembly of tiny particles. To establish such special synthetic conditions in the CdTe system, not only are its typical features and possible solutions deeply analyzed, but also related factors, such as the ligand environment, injection and growth temperature, and Cd-to-Te precursor ratio, are systematically investigated. High-quality ultralong (up to 10 μm) and ultrathin (less than 10 nm) CdTe nanowires are produced in solution under optimal reaction conditions. Morphological, spectral, and compositional analyses are performed to examine the products formed at different reaction stages in order to clarify the formation mechanism of the CdTe nanowires. Furthermore, the transformation of the CdTe nanowires into CdTe/CdSe core–shell heterostructures is intensively explored, and the CdSe epitaxial growth process is specially tracked by morphological and spectral characterization techniques. Finally, CdTe nanowires coated with a continuous and dense CdSe shell are successfully fabricated by using a proper coating protocol.

1. Introduction

Semiconductor nanocrystals (SNCs) have attracted much attention in recent years due to their unique size-, shape- and composition-dependent optical and electrical properties, as well as their promising applications in various fields. Among different types of SNC, ultralong (on the micrometer scale) and ultrathin (less than 10 nm) semiconductor nanowires (SNWs)

are of particular importance in fabricating nanoscale electronics,^[1] solar cells,^[1c,1d,2] nanolasers,^[1d,3] photodetectors,^[1d,4] and chemical sensors,^[1c,1d,5] owing to the unique physical and chemical properties associated with their high dimensional anisotropy. As one class of important SNWs, CdTe nanowires not only have excellent optical response properties (such as high absorption coefficient and broad absorption region) but also possess good carrier transport ability; therefore they are ideal candidates for the above-mentioned applications. However, until now, it has been a challenge to synthesize high-quality (high purity, good crystallinity, uniform morphology) ultralong and ultrathin CdTe nanowires, although quite a few methods^[6] (including a template-assisted approach,^[7] chemical vapor deposition (CVD),^[8] the solution–liquid–solid (SLS) method,^[9] the solvothermal method,^[10] a ligand-induced strategy,^[11] and solution-based oriented attachment strategy^[12]) have been developed. Among those methods, it seems the solution-based SLS and oriented attachment ones are promising candidates to solve the challenge of synthesis of high-quality CdTe NWs. In fact, the SLS method is a general strategy to produce high-quality II–VI and III–V SNWs in solution. Buhro's^[9a,9b] and Kuno's^[9c,9d] groups have recently prepared high-quality CdTe nanowires by utilizing the SLS method. However, the adoption of Bi nanoparticles (or Bi salts) as the necessary catalyst in the SLS method not only complicates the synthetic protocol but also contaminates the as-prepared CdTe nanowires products. As for the oriented attachment strategy, although this particular growth regime is not yet fully understood it does show some fascinating advantages in the preparation of high-quality SNWs. For example, several groups have demonstrated that high-quality PbSe and ZnTe nanowires can be formed through an oriented attachment route if some special reaction conditions (such as *in situ* formation of tiny particles, strong dipole–dipole interactions, an overall weak coordinating environment, and relatively high reaction temperature) meet in that reaction system.^[6b,12b,12e–12g,13] However, the above features do not always hold true in the cases that oriented attachment takes effect. For example, Kotov's group^[12a,12d] has impressively

F. Jiang, J. J. Liu, Prof. Y. C. Li, Prof. L. Z. Fan

Department of Chemistry
Beijing Normal University
Beijing, 100875, P. R. China
E-mail: liyc@bnu.edu.cn

Dr. Y. Q. Ding, Prof. Y. F. Li
Beijing National Laboratory for Molecular Sciences
CAS Key Laboratory of Organic Solids
Institute of Chemistry
Chinese Academy of Sciences
Beijing 100190, P. R. China
E-mail: liyf@iccas.ac.cn

DOI: 10.1002/adfm.201102800



demonstrated that CdTe nanoparticles can be slowly assembled into straight nanowires at room temperature after removing ligands from their surfaces. Nevertheless, it should be pointed out that the formation of CdTe nanowires in such case is typically time-consuming and low efficiency. Therefore, in order to obtain high-quality CdTe nanowires, straightforward thinking suggests a strategy of building up reaction conditions similar to those used in the preparation of PbSe and ZnTe nanowires; unfortunately, such special reaction conditions are hard to copy from one system to another.

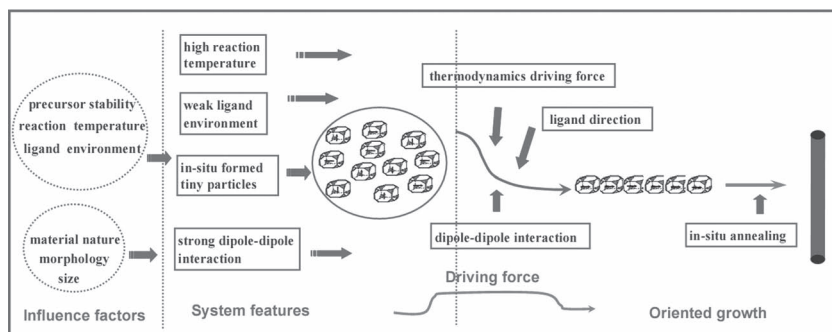
A big problem associated with SNWs is the existence of many defects on their surfaces, which will significantly deteriorate their optical, electrical and thermodynamic performance. To solve this problem, the core–shell modification technique (i.e., coating a shell of another material onto the surfaces of SNWs) has been introduced, which also turns out to be a powerful approach to tune the overall physical and chemical properties of SNWs.^[14] Therefore, great effort has been made to synthesize various SNWs with core–shell structures.^[15] CdTe/CdSe core–shell nanowires, as a novel class of heterostructures, are expected to have not only a quite broad optically active region (even broader than that of CdTe and CdSe) but also the ability to automatically separate and efficiently transport the holes and electrons photogenerated in them. Thus, such heterostructured nanowires show great promise for application in a new generation of optoelectronic devices, and have attracted strong interest from both the scientific and industrial community.^[14c,14e,15a] However, until now, trials to coat CdTe nanowires with a homogeneous CdSe shell have not succeeded, probably owing to the relatively large lattice mismatch (around 7%) between these two materials, as well as additional difficulties associated with the morphological anisotropy of the core nanowires.^[14d,14e,16] Therefore, to solve the challenges, the coating protocol (including shell-growth strategy, precursor reactivity, ligand environment, and reaction temperature) need to be fully optimized to allow the overgrowth of CdSe shells on CdTe nanowires in a more controllable and uniform way.

Herein, we present a novel catalyst-free synthetic strategy for growing high-quality CdTe nanowires in solution, based on the building up of special reaction conditions to allow nanowire formation through oriented assembly of tiny particles formed *in situ*. To establish such special conditions, we not only deeply analyzed the system's typical features and possible solutions, but also systematically investigated the influence of several related factors. Meanwhile, we employed spectral and morphological analysis to examine the products formed at different reaction stages in order to clarify the formation mechanism of the CdTe nanowires. Furthermore, we achieved coating of CdTe nanowires with a uniform shell of CdSe, by using an optimal coating protocol. To our knowledge, this is the first time to intentionally construct and employ oriented attachment to produce ultralong and ultrathin CdTe nanowires in solution, and is also the first time uniform CdTe/CdSe core–shell nanowires have been obtained through a wet-chemical route.

2. Results and Discussion

2.1. Optimal Reaction Conditions for Growing CdTe Nanowires in Solution

As described above, the identification of special reaction conditions similar to those used for the synthesis of PbSe^[12b] and ZnTe^[12e,12f] nanowires would provide the possibility of producing high-quality CdTe nanowires through oriented attachment. To reach this goal, we first need to answer two basic questions: what features must such special reaction conditions possess and how should such special reaction conditions be built up in the CdTe reaction system? Based on successful examples achieved in the past,^[12b,12e,12f,13] the first question has been answered in the Introduction; a system under such special reaction conditions typically has the following features: i) there are thousands of tiny particles coexisting in the system at that moment, ii) there are strong dipole–dipole interactions between nanoparticles, iii) only a small amount of coordinating ligands is present in the reaction environment, and iv) the reaction is typically carried out at relatively high temperature (higher than 250 °C) and can be performed in a few minutes (see Scheme 1). Obviously, to answer the second question, we first need to understand the exact nature of these features. As shown in Scheme 1, the first feature can result from explosive nucleation and therefore has a close relationship with precursor stability, ligand environment, and reaction temperature. The second one is attributed to asymmetrical arrangement of polar facet on particle surface and thus is closely related to the material nature, morphology, and size of these particles. The final two features relate to the ligand environment and reaction temperature, respectively, and thus are easy to produce; in fact, these features are not too particular and could be available in many reaction systems. The real challenge lies not only in these features being hard to maintain in a real system due to violent reactions but also in their standard levels not yet being clear. As a result, the special reaction conditions that lead to oriented attachment are generally hard to copy from one system to another and need systemic investigation to determine. Based on this analysis, to obtain such special reaction conditions in the CdTe reaction system (the second question), we will focus our investigation on the influence of the ligand environment, the injection and growth temperature, and the Cd-to-Te precursor ratio, which together fully cover the four features required.



Scheme 1. Sketch highlighting special reaction conditions under which the formation of nanowires through oriented attachment is possible.

2.1.1. Influence of the Ligand Environment

It is well-known that the ligand environment not only plays a key role in determining precursor reactivity but also has a direct influence on the nucleation, growth, and assembly of nanocrystals.^[17] Therefore, it is of particular importance to find a suitable ligand environment in order to grow CdTe nanowires using an oriented attachment strategy. To do so, we choose trioctylphosphine oxide (TOPO), stearic acid (SA) plus tetradecylphosphonic acid (TDPA), and trioctylphosphine (TOP) as the bulk solvent, the coordinating ligand for Cd, and the coordinating ligand for Te, respectively, based on previous experience.^[9,18] Moreover, we carried out a systemic investigation on the influence of TDPA concentration to obtain an optimal ligand environment. As shown in **Figure 1**, it was found that TDPA does exert an important influence on the morphology of the as-prepared CdTe nanocrystals. For example, when TDPA was absent in the reaction environment, only tiny branched CdTe nanorods (ca. 8 nm long and 4 nm wide) were formed (see **Figure 1a**). As the TDPA concentration was increased to 0.05 g mL⁻¹, uniform CdTe nanowires (ca. 6.0 μm long and 6.5 nm thick) were produced (see **Figure 1b**). When the TDPA concentration was further increased to 0.1 g mL⁻¹, CdTe nanowires together with branched nanorods were obtained, although the former was the major product (see **Figure 1c**). When the TDPA concentration was finally increased to 0.14 g mL⁻¹, CdTe branched nanorods (ca. 20 nm long and 6 nm thick) became the major product (see **Figure 1d**). We think the TDPA-mediated growth phenomenon may be attributed to the TDPA exerting multiple influences on the growth of CdTe nanocrystals, with the nature of the influence having a close relationship with the amount of TDPA in the ligand environment. According to previous studies, the

influences of TDPA may include: determining the reaction reactivity of Cd precursors (dependent on TDPA-to-Cd molar ratio), facilitating 1D growth of CdTe nanocrystals through selectively binding,^[18] and affecting the cleavage rate of alkyl-phosphine chalcogenide bonds (P=Te).^[19] With the increase of TDPA amount in the ligand environment, the above influences will be all enhanced but may be contrary to the growth of CdTe nanowires. For example, the influence of TDPA on Cd precursor and on P=Te cleavage have opposing effects in terms of the nucleation rate and growth rate. Therefore, CdTe nanowires are only formed in a specific ligand environment with limited TDPA content, in which the influences of TDPA can achieve a good balance.

2.1.2. Influence of Injection and Growth Temperature

It has been demonstrated previously that injection temperature and growth temperature are two important parameters that, respectively, affect the nucleation and growth of nanocrystals in solution.^[18b,18c,18d] Therefore, we systematically varied injection and growth temperature in the preparation of CdTe nanocrystals in order to characterize these influences. As shown in **Figure 2**, the variation of injection and growth temperature does significantly change the morphologies of the as-prepared CdTe nanocrystals (the ligand environment was kept constant, 6 mL TOPO plus 0.3 g TDPA). For example, when injection and growth temperatures were set at 310 and 280 °C, respectively, CdTe nanowires were formed along with a small amount of flower-like product (see **Figure 2a**); when the injection temperature was lowered to 300 °C and the growth temperature kept at 280 °C, high-quality CdTe nanowires were the major product (see **Figure 2b**). As injection temperature was kept at 300 °C but growth temperature lowered to 270 °C, CdTe branched nanorods became the main product (see **Figure 2c**). When the injection and growth temperature were further lowered to 270 and 260 °C, respectively, only a low yield of CdTe nanowires was obtained and most of the Cd precursor was found to be unreacted (see **Figure 2d**). Generally speaking, a relatively high injection temperature favors the formation of sufficient nuclei in solution through explosive nucleation; however, if the injection temperature is set too high or too low, the nucleation step will be out of control. On the other hand, relatively high growth temperature can not only offer a strong driving force for growth or assembly of nanocrystals, but also provide an opportunity to dynamically vary the surface polarity of nanocrystals through violent surface reactions (facilitating the dipole moment formation in nanocrystals).^[12b] Because the nucleation, growth, and assembly process were carried out in parallel in this case, a small difference between injection and growth temperatures must be maintained in order to achieve a good balance between

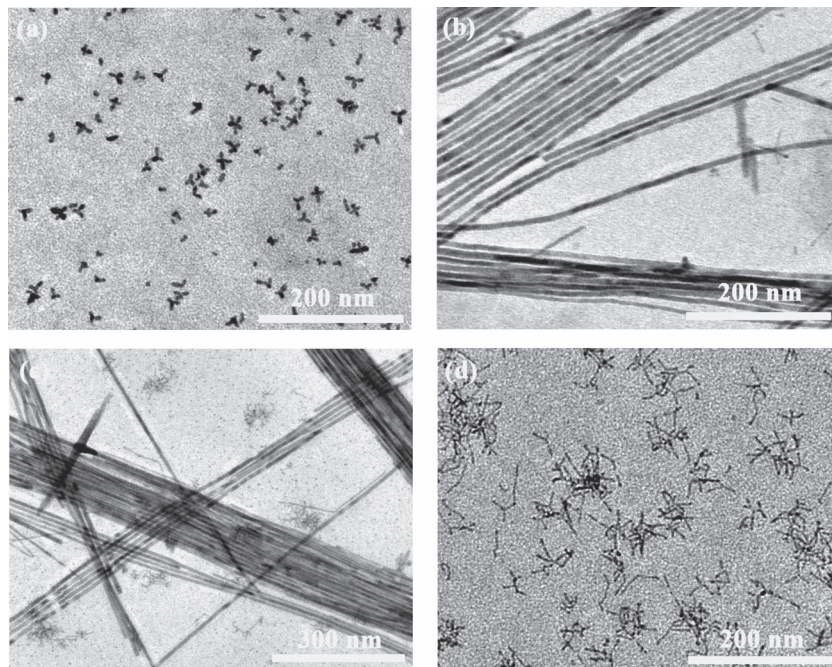


Figure 1. TEM images of CdTe nanocrystals prepared in a hot TOPO solution containing different concentrations of TDPA: a) 0 g mL⁻¹ b) 0.05 g mL⁻¹, c) 0.1 g mL⁻¹, and, d) 0.14 g mL⁻¹.

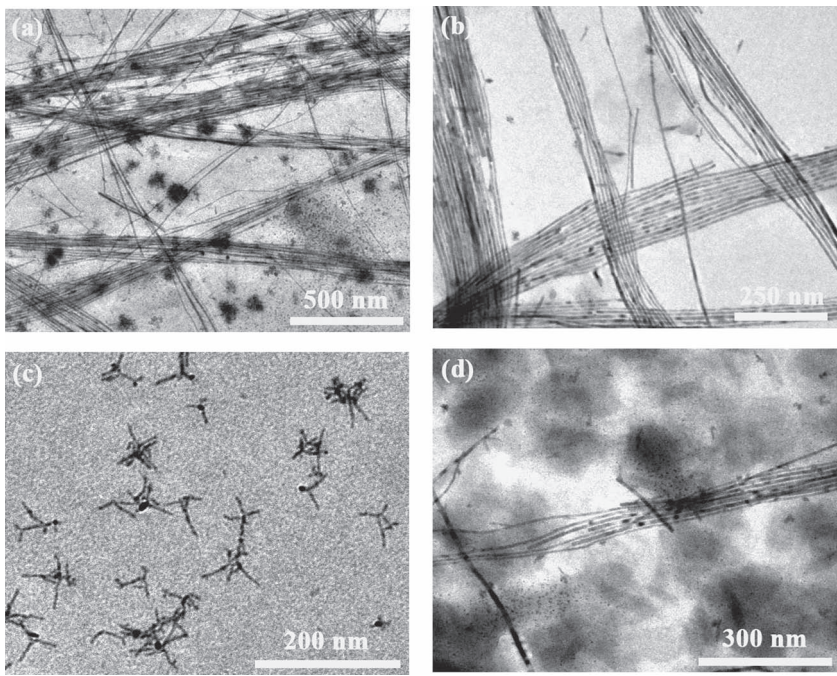


Figure 2. TEM images of CdTe nanocrystals prepared in the same solvent but at different injection and growth temperatures: a) injection at 310 °C and growth at 280 °C, b) injection at 300 °C and growth at 280 °C, c) injection at 300 °C and growth at 270 °C, and, d) injection at 270 °C and growth at 260 °C.

them. It therefore seems that relatively high injection and growth temperatures are necessary to form CdTe nanowires in solution and the reaction can only be carried out successfully in a quite narrow temperature range.

a much higher Cd-to-Te ratio is required in the growth of CdTe nanowires. A possible explanation is that a higher Cd-to-Te ratio favors enhancement of the surface polarity of the CdTe nuclei and provides an additional driving force for their assembly in solution.

Based on these results, we can now build up the optimal reaction conditions for growing CdTe nanowires through oriented attachment of tiny particles formed *in situ*. These are: a rapid injection of TOPTe (0.2–0.4 mmol) into a mixed solvent containing TOPO (5.0–6.0 g), TDPA (0.3–0.6 g), and Cd(Ac)₂ (2–4 mmol) at 280–300 °C, and carrying out the reaction at 280–290 °C for 1–5 min.

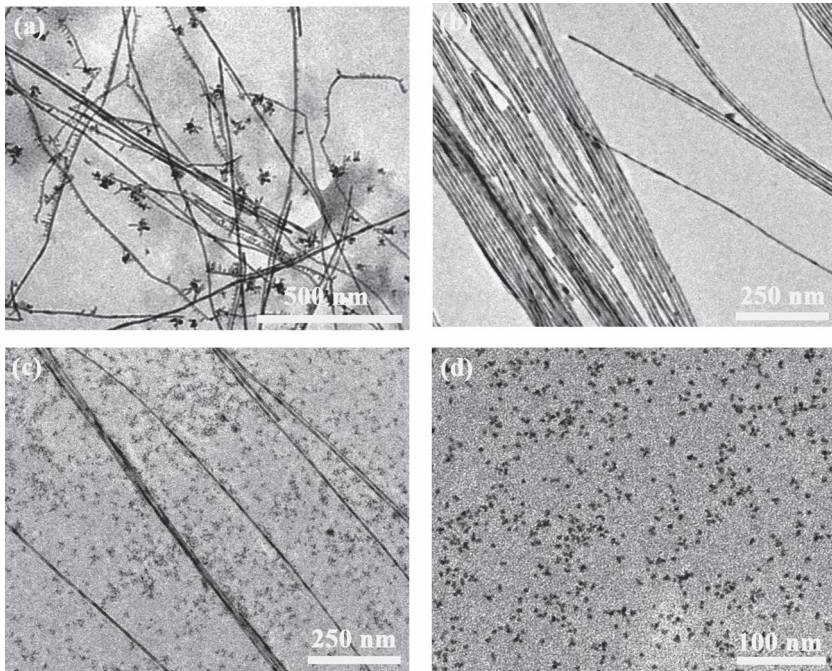


Figure 3. TEM images of CdTe nanocrystals prepared under identical conditions except for using different Cd-to-Te molar ratios: a) 10:1, b) 10:1.5, c) 10:2.5, and, d) 10:4.

2.2. Characterization of CdTe Nanowires

Under the optimal reaction conditions, high-quality CdTe nanowires were produced in solution, as expected. As a typical example shown in Figure 4, the resulting CdTe nanowires demonstrate excellent qualities, such as uniform morphology, high purity, good crystallinity, very long length, and very thin thickness. TEM and SEM images (Figure 4 and Figure S1 in the Supporting Information) both reveal that these nanowires are not only quite uniform in thickness (less than 10 nm thick) and length (up to 10 μm long),

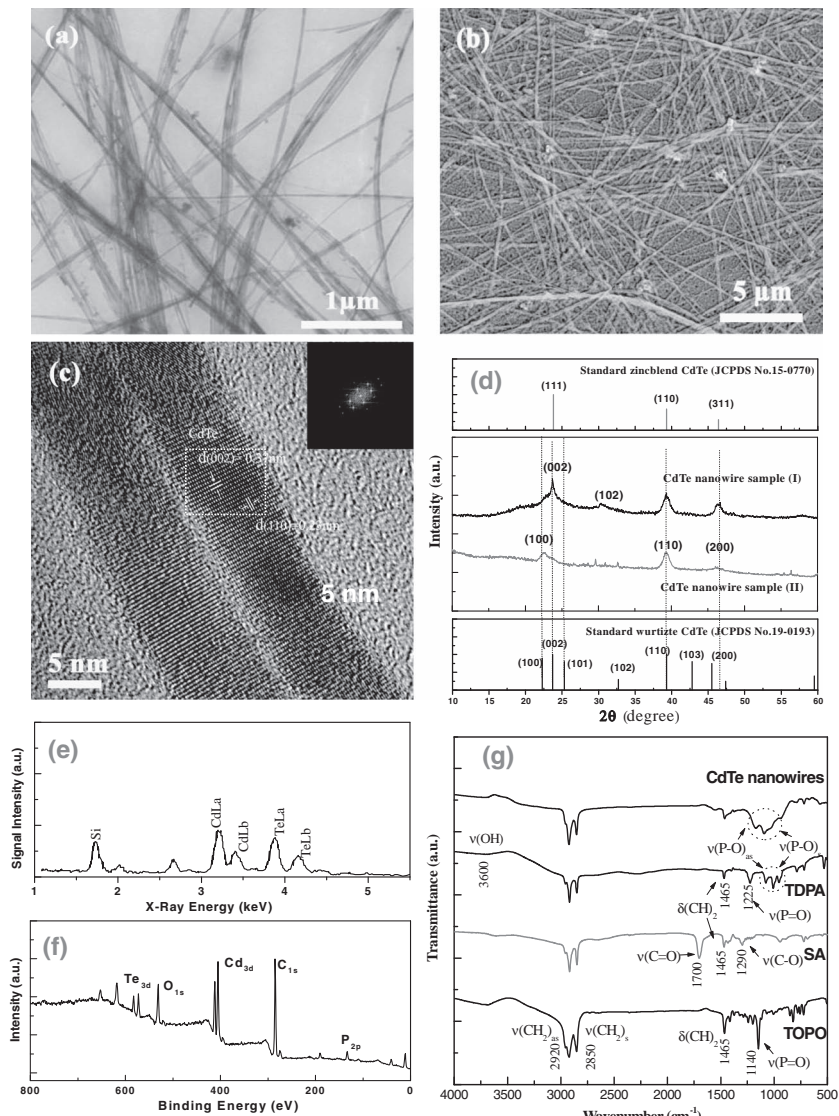


Figure 4. TEM image (a), SEM image (b), HRTEM image (c), XRD patterns (d), EDS spectrum (e), XPS spectrum (f), and FTIR spectra (g) of the CdTe nanowires typically obtained under optimal reaction conditions. The inset in (c) is the FFT pattern of the area marked therein. Sample I in (d) is CdTe nanowires in powder form while Sample II is CdTe nanowires drop-cast on a Si substrate. The TOPO, SA, and TDPA labeled in (g) are the pure ligands, for comparison purposes.

but also are produced in high yield and bundle together in the final product. It should be pointed out that their thickness and length have found to be related to reaction time, and thus can be easily modulated (Figure S1 and S6 in the Supporting Information). HRTEM images (Figure 4c) together with corresponding fast Fourier transform ED (FFT ED) demonstrate that these nanowires are single crystals with a wurtzite structure, having interplanar spacings of 0.37 nm for (002) planes and 0.23 nm for (110) planes. Moreover, the HRTEM image also unveils these nanowires growing along the [001] direction, which is quite different from the nanowires obtained at room temperature.^[12a,12d,12g] XRD patterns (Figure 4d) further confirm that these nanowires have hexagonal wurtzite structures

by giving characteristic (100), (002), and (101) peaks. It should be pointed out that some peaks are found to be enhanced while others are suppressed (even disappearing) compared to bulk wurtzite CdTe patterns. These changes are quite obvious in the case that CdTe nanowires are drop-cast on a Si substrate, and thus can be attributed to substrate-induced nanowire orientation.^[9c] EDS and XPS (Figure 4e and f) both reveal the atomic ratio of Cd-to-Te in these nanowires is close to 1:1, which is in good agreement with the stoichiometric ratio in CdTe, indicating the high-purity nature of them. FTIR spectra (Figure 4g and Figure S2 in the Supporting Information) together with XPS spectra (Figure 4f and Figure S3 in the Supporting Information) confirm TDPA is the major ligand for CdTe nanowires, although TOPO and SA are the main ligands in the reaction environment. It should be noted that no peak from CdO or TeO₂ is detected in the Cd_{3d} and Te_{3d} XPS spectrum (Figure S3 in Supporting Information), implying these nanowires could be stable in air (at least for one or two days) with TDPA protection.

2.3. The Mechanism for Catalyst-Free Growth of CdTe Nanowires From Solution

To confirm our assumption regarding the formation mechanism of CdTe nanowires, we employed morphological, spectral, and compositional analysis to examine the products formed at different reaction stages and to record their corresponding changes with time. As shown in Figure 5a–e, TEM images clearly reveal the morphological evolution of CdTe nanocrystals during their growth. Upon injection of Te precursor, a large amount of CdTe tiny particles (“clusters”) with wurtzite structures (see Figure 5a and Figure S7 in the Supporting Information) were formed simultaneously, with their average diameters rapidly reaching 3.4 nm only 5 s after the

injection. Very impressively, only 25 s later, some extremely long nanowires with an average diameter of 6.5 nm showed up (see Figure 5b). The transformation from particle to nanowire dominated with the increase of reaction time, and high-quality nanowires (average 7.5 nm in diameter) were found to be the major product as the reaction proceeded for only 1 min (see Figure 5c). With further prolongation of reaction time (from 1 to 10 min and then to 20 min), no obvious morphological changes except for slight variation in the thickness (from ca. 7.5 to 8.0 nm and then ca. 12 nm) and length were observed for the resulting CdTe nanowires (see Figure 5c–e and Figure S5 and S6 in the Supporting Information). Such changes in thickness and length probably arise from the thermodynamic instability

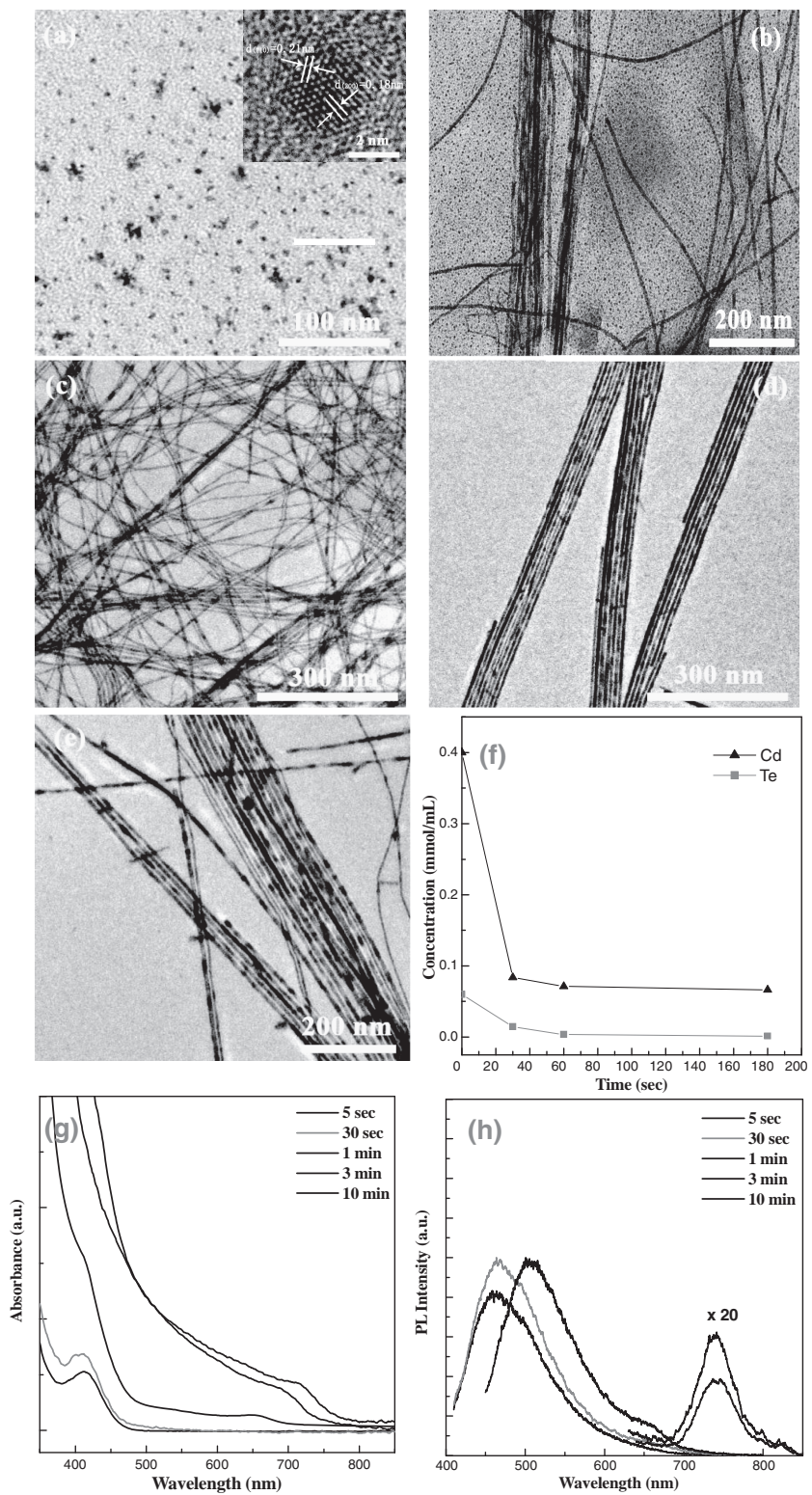


Figure 5. TEM images showing the morphological evolution of the CdTe nanocrystals formed at different reaction time during CdTe nanowire formation: a) 5 s, b) 30 s, c) 1 min, d) 3 min, and e) 10 min. f) Temporal evolution of the remaining Cd and Te precursor concentration in the reaction solutions after injection. g,h) Temporal evolution of the absorption spectra (g) and the photoluminescence spectra (h) of the CdTe nanocrystals formed at different reaction time.

of the nanowires at high temperature. It should be noted that the color of the samples taken at different reaction stages also demonstrates an evolution with time (from yellow to light brown and then to dark brown, see Figure S4 in the Supporting Information), unveiling the above morphological evolution of the CdTe nanocrystals from another standpoint. Meanwhile, the variation of the remaining Cd and Te concentration in the reaction environment with time was measured by inductively coupled plasma (ICP) atomic emission spectroscopy. As shown in Figure 5f, the remaining Cd and Te concentrations were found to be maintained at a very low level and remained almost constant after injection, which indicates that the nanowires were formed by consuming the preformed nanoparticles rather than the free precursors. At the same time, the temporal evolution of absorption and photoluminescence spectra were utilized to track the growth of nanocrystals in solution. Figure 5g and h show the absorption and photoluminescence (PL) spectra obtained at 5 s; the sharp absorption peak around 420 nm (absorption edge around 470 nm) in the absorption spectrum and the emission peak around 450 nm in the PL spectrum definitely manifest the formation of many “clusters” at the early stage. According to the Wang equation, this absorption peak can be assigned to the first excitonic transition of CdTe nanoparticles with a diameter of 3.3 nm,^[20] which agrees well with the TEM observations. Furthermore, with the prolongation of reaction time, it was found that the absorption peak around 420 nm and the emission peak around 450 nm (both come from the preformed particles) rapidly disappeared, while a new absorption peak around 650 nm and a new emission around 750 nm (both come from the nanowires) showed up. Such spectral changes imply that the amount of tiny particles in solution decreased while the amount of the nanowires increased as the reaction proceeded.

It should be pointed out that the formation of many clusters at the early stage as well as their rapid replacement with superlong nanowires at the following stage strongly support the nanowires being grown according to the oriented attachment mechanism. In addition, the fact that the average diameter of the initially formed nanowires is about two times larger than that of the preformed clusters indicates the radial packing of these particles (two-particle side-by-side combination) is inevitable during their axial packing process.^[12b,12h]

2.4. High-Yield Transformation of CdTe Nanowires into CdTe/CdSe Core–Shell Heterostructures

As mentioned above, coating CdTe nanowires with a shell of CdSe may offer some fascinating optoelectronic properties; however, until now it has been a challenge for synthesis of such heterostructures. Here we performed an alternative dropwise addition of shell precursors of proper reactivity, selecting

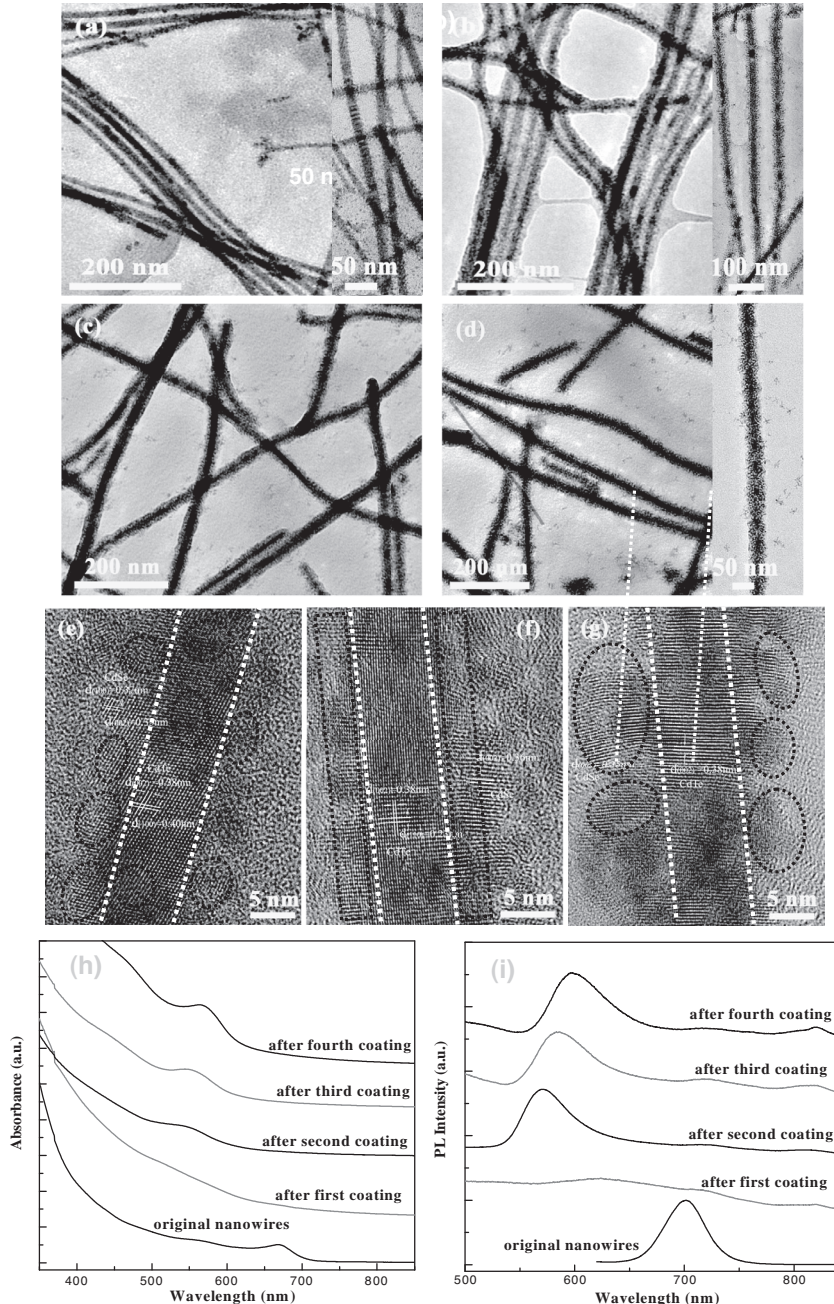


Figure 6. Temporal evolution of TEM images (a–d), HRTEM images (e–g), absorption spectra (h), and photoluminescence spectra (i) of CdTe/CdSe core–shell nanowire samples collected at different stages during CdSe shell growth. (a–d) are the TEM images of CdTe/CdSe nanowires after the 1st, 2nd, 3rd, and 4th injection of CdSe precursors, respectively. (e–g) are the HRTEM images corresponding to (a), (b), and (d), respectively.

noncoordinating ODE as the reaction solvent and 200 °C as the coating temperature to allow the overgrowth of CdSe shells on CdTe nanowires in a more controlled way (see the primary results in Figure S8 and S9 in the Supporting Information). Moreover, we also carried out systemic investigation of the CdSe coating process to figure out its epitaxial growth characteristics. As a representative example, **Figure 6** shows the temporal evolution of TEM images, and absorption and photoluminescence spectra of CdTe/CdSe nanowire samples collected at different stages during CdSe shell growth.

As shown in Figure 6a, upon the first addition of a specified amount of CdSe shell precursor into a solution containing CdTe nanowires at 200 °C, the surfaces of the nanowires are found to be much rougher than the original. A closer inspection (the inset in Figure 6a) reveals that the nanowires are actually decorated with many tiny particles. The HRTEM image (Figure 6e) together with the EDS spectrum (Figure S10 in the Supporting Information) further reveals that the tiny particles are wurtzite CdSe and are randomly distributed on the surfaces of CdTe nanowires. After the specified amount of CdSe shell precursors was introduced into the solution again (the second injection), most of the nanowires are found to be overcoated with a continuous and dense CdSe shell. More detailed observation reveals that such CdSe shells are composed of many tiny CdSe nanorods (ca. 2 nm in width and 8 nm in length), and therefore they look like tiny bristles attaching on CdTe nanowires. More importantly, the HRTEM image (Figure 6f) confirms that the CdSe shells epitaxially coat the CdTe nanowires and the innermost several monolayers are almost continuous integrated with the core nanowires, which indicates the epitaxial growth of CdSe on CdTe nanowires may follow the Stranski-Krastanow mode.^[15d,21] With the addition of more CdSe shell precursors into the solution (the third and fourth injections), the overall CdSe shells as well as the inner CdSe nanorods are both found to become thicker, which makes the core–shell nanowires quite resemble nanoscale thorns. It should be pointed out that the formation of such thorn-like architectures upon overcoating CdTe nanowires with CdSe implies two facts: one is the interface strain in this case should be quite large and thus the Stranski-Krastanow epitaxial growth mode is favorable; the another is that the growth of the CdSe shell is probably under a kinetically controlled regime and therefore results in such an anisotropic growth. In term of core–shell architecture, the interface strain is believed to be related to the thickness

ratio between the core and the shell as well as to the crystallographic difference between the two materials^[14d,e]; while the shell growth regime is thought to be dependent on the reaction conditions (such as shell precursor concentration, amount, reactivity and its injection rate).^[15f] Meanwhile, temporal evolution of absorption and photoluminescence spectra recorded the coating process from another point of view. As shown in Figure 6h and i, during CdSe shell growth, the absorption peak at 670 nm and the emission peak at 700 nm (both from the core nanowires) are both quickly smeared out (after the first addition of CdSe shell precursor), while a new absorption peak around 550 nm and emission peak around 570 nm (which can be assigned to the absorption and emission of CdSe nanorods in the shells based on TEM results) gradually show up and are red-shifted slightly (after the second addition of CdSe shell precursor). It should be noted that the loss of characteristic absorption and emission peak of CdTe nanowires is a direct proof to support Type II core–shell structures already being formed at that moment. (i.e., after the first coating).^[22] Moreover, the absorption and emission peaks from the CdSe shells become dominated and red-shifted with the increase of CdSe shell precursor, indicating that the feeding precursors are mainly consumed by the preformed CdSe nanorods rather than new ones produced since then (i.e., after the second coating). Additionally, this fact also implies that the shell precursor amount may influence the shell growth mode during the coating process.

Based on these investigations, it is evident that the adoption of proper coating reaction condition (such as employing proper reactive precursor, slow and alternative precursor injection, rational precursor injection amount, medium coating temperature, and weak ligand environment and proper post-treatment) along with careful selection and purification of the core nanowires is of particular importance in forming a uniform shell on the nanowires. Therefore, more efforts should be made to establish the optimal coating protocol in order to obtain high-quality CdTe/CdSe or other type of core–shell nanowires; this research goal is being actively pursued by our group.

3. Conclusions

We report a novel catalyst-free synthetic strategy for the growth of high-quality CdTe nanowires in solution, by constructing a special reaction condition to allow nanowires formation through oriented assembly of tiny particles formed *in situ*. To establish such reaction conditions, we not only analyzed its typical features and possible solutions, but also systematically investigated the influence of several important factors (such as ligand environment, injection and growth temperature, and Cd-to-Te precursor ratio) on the growth of CdTe nanowires. High-quality CdTe nanowires were been produced by using this synthetic strategy under optimal reaction conditions. Meanwhile, we performed morphological, spectral, and compositional analysis to confirm our assumptions about the formation mechanism of CdTe nanowires. The results revealed that many clusters were formed at the early stage and nanowires were then produced at the cost of consuming the preformed clusters, which strongly supports the oriented attachment growth mechanism of the CdTe nanowires. Furthermore, we have demonstrated the

transformation of CdTe nanowires into CdTe/CdSe core–shell heterostructures could be finally done by using a proper coating protocol. Morphological along with spectral analysis confirmed most of the nanowires are overcoated with a continuous and dense CdSe shell after injection of enough shell precursors. We believe that the synthesis and coating strategy demonstrated in this paper will throw an attractive light on how to prepare high-quality SNWs catalyst-free in solution as well as how to transform them into core–shell heterostructures at high yield.

4. Experimental Section

Materials: Methanol, ethanol, chloroform, toluene, stearic acid (SA), and cadmium acetate ($\text{CdAc}_2 \cdot 2\text{H}_2\text{O}$) at analytical grade were purchased from Beijing Chemical Reagent Co. Ltd. of China. Tellurium powder (99.8%, 200 mesh), selenium powder (99.999%, 200 mesh), trioctylphosphine (TOP, tech. 90%), trioctylphosphine oxide (TOPO, 98%), and 1-octadecene (ODE, tech. 90%) were purchased from Alfar. Hexadecylamine (HDA, 96%) and *n*-tetradecylphosphonic acid (TDPA, 96%) were purchased from Aldrich and PCI Synthesis, respectively. Cadmium acetate was dried completely before use, and other reagents were used as received.

Synthesis of CdTe Nanowires: Generally, CdTe nanowires were prepared by using a hot-injection method and were carried out with stirring and in an inert atmosphere utilizing a standard air-free technique. To prepare CdTe nanowires, 2.0–3.0 mmol CdAc_2 , 4.0–6.0 mmol SA, a specified amount of TDPA, and 5.0 g TOPO were first added into a 25 mL three-neck flask. The mixture was heated to form a clear solution and was then fixed at a specified temperature (typically higher than 250 °C). Freshly prepared 1.0–2.0 mL TOP-Te (containing a specified amount of Te) was swiftly injected into this solution. After injection, the system was generally dropped tens of degrees (depending on TOP injection volume) and was kept at that temperature for 1–10 min (Protocol A). To obtain the optimal condition for growth of CdTe nanowires, various amount of TDPA (0, 0.3, 0.6, or 0.8 g), different injection/reaction temperatures (310/280, 300/280, 300/270, 275/265 °C), and different Cd/Te ratios (2/0.2, 2/0.3, 2/0.6, 2/0.8) were tested.

Synthesis of CdTe/CdSe Core–Shell Nanowires: To fabricate CdTe/CdSe core–shell nanowires, pre-purified CdTe nanowires (ca. 30 mg) dissolved in toluene were added into a three-neck flask (containing 6 mL ODE) as the templates and heated to 200 °C in a N_2 atmosphere. Then, a specified amount of Cd and Se precursor (for example, 0.1–0.2 mmol $\text{Cd}(\text{Ac})_2$ and Se dissolved in 2 mL TOP) were alternately, repeatedly (depending on target shell thickness) and dropwise (ca. at 0.1 mL min⁻¹) injected into such solution. The interval between two continuous injections was typically longer than 5 min. The shell thickness is dependent on the precursor injection total amount (i.e., injection time × the amount of per injection) and the size (the length and the thickness) of the core nanowires, and their relationship can be described by a cylinder model^[23] (Protocol B). To obtain the optimal conditions for growth of CdSe shell on CdTe nanowire, various types ligand solvent (TOPO, ODE, TOPO+HDA) and different coating temperatures (140, 200, 240 °C) were tried.

Purification of Nanocrystal Products: After reaction, the colloid solutions obtained in the above experiments (from Protocol A to Protocol B) were cooled, and precipitated by acetone (or methanol). The formed flocculent precipitate was centrifuged and the upper layer liquid was decanted, then the isolated solid was dispersed in toluene (or chloroform). The above centrifugation and isolation procedure was repeated several times for purification of the nanocrystals (Protocol C). Finally, the purified nanocrystals were re-dispersed in toluene (or chloroform) for use in coating reaction (Protocol B) or for the preparation of TEM and SEM specimens or dried under vacuum for characterization by XRD, XPS and FTIR spectroscopy. It should be pointed out that the nanowires samples for use in coating reaction or for XPS characterization need to be handled in an inert atmosphere to avoid oxidization.

Characterization of Nanocrystal Products: For measurement of the absorption and PL spectra of the CdTe or CdTe/CdSe nanowires formed at a given time, a needle-tip aliquot was taken from a reaction flask and dissolved in toluene (or chloroform). UV-vis absorption spectra were recorded on a Hitachi U-3010 spectrophotometer, while PL spectra were measured on a Hitachi U-4500 spectrophotometer. Infrared spectra were recorded on a PE2000 FTIR with 4 cm⁻¹ resolution. To measure the remaining Cd and Te concentration in a synthetic system, inductively coupled plasma atomic emission (ICP) was employed to analyze the aliquots taken from the reaction flask at a given moment; the aliquots must suffer from a standard HCl/HNO₃ digestion before ICP measurements. Scanning electron microscopy (SEM) characterization was done by using a HITACHI S-4800 scanning electron microscope with X-ray energy dispersive spectroscopy (EDS). Transmission electron microscopy (TEM) observations were performed with a JEOL JEM-1011 transmission electron microscope. High-resolution transmission electron microscopy (HRTEM) and selected area electron diffraction (SAED) measurements were carried out using a JEOL JEM-2100F transmission electron microscope operated at 300 kV. The specimens for TEM observation were prepared by depositing a drop of a dilute toluene solution of CdTe or CdTe/CdSe nanocrystals on a carbon-coated copper grid and drying at room temperature. The SEM specimens were prepared by adding drops of dilute solution of CdTe or CdTe/CdSe nanowires on Si substrates. X-ray diffraction (XRD) patterns were recorded by a Rigaku D/max-2400 diffractometer operated at 40 kV and 200 mA current with Cu K- α 1 radiation. XPS data were obtained on a VG-Scientific ESCA Lab 220i-XL spectrometer equipped with a hemisphere analyzer and using Al K α X-ray as excitation source. The samples for XRD and XPS measurements were solid powder prepared by drying some purified products under vacuum. For comparison, some CdTe nanowire powders were dispersed in toluene and drop-casted on a Si substrate for XRD characterization. The samples for FTIR spectroscopy were prepared by dispersing CdTe nanowires or pure ligands in a KBr pellet.

Supporting Information

Supporting Information is available from the Wiley Online Library or from the author. It includes TEM images, size distribution histograms, and XPS spectra of CdTe nanowires; optical images, TEM images, and XRD patterns of the CdTe products formed at different reaction stages (time) in CdTe nanowires formation; and TEM images and EDS spectra of CdTe/CdSe complex prepared under different conditions.

Acknowledgements

This work was supported by the National Natural Science Foundation of China (NSFC, nos. 21003012 and 91023039), the Beijing National Laboratory for Molecular Sciences (BNLMS) of China and the Scientific Research Foundation of Beijing Normal University.

Received: November 21, 2011
Published online: March 19, 2012

- [1] a) Y. Huang, X. Duan, Y. Cui, L. J. Lauhon, K.-H. Kim, C. M. Lieber, *Science* **2001**, *294*, 1313; b) Y. Li, F. Qian, J. Xiang, C. M. Lieber, *Mater. Today* **2006**, *9*, 18–27; c) B. A. Korgel, *AIChE J.* **2009**, *55*, 842–848; d) P. D. Yang, R. X. Yan, M. Fardy, *Nano Lett.* **2010**, *10*, 1529–1536.
- [2] a) B. Z. Tian, X. L. Zheng, T. J. Kempa, Y. Fang, N. F. Yu, G. H. Yu, J. L. Huang, C. M. Lieber, *Nature* **2007**, *449*, 885–889; b) K. S. Leschkies, R. Divakar, J. Basu, E. Enache-Pommer, J. E. Boercker, C. B. Carter, U. R. Kortshagen, D. J. Norris, E. S. Aydil, *Nano Lett.* **2007**, *7*, 1793–1798; c) K. Yu, J. Chen, *Nanoscale Res. Lett.* **2009**, *4*, 1–10.

- [3] a) M. H. Huang, S. Mao, H. Feick, H. Q. Yan, Y. Y. Wu, H. Kind, E. Weber, R. Russo, P. D. Yang, *Science* **2001**, *292*, 1897–1899; b) X. F. Duan, Y. Huang, R. Agarwal, C. M. Lieber, *Nature* **2003**, *421*, 241–245.
- [4] a) C. Soci, A. Zhang, B. Xiang, S. A. Dayeh, D. P. R. Aplin, J. Park, X. Y. Bao, Y. H. Lo, D. Wang, *Nano Lett.* **2007**, *7*, 1003–1009; b) C. Soci, A. Zhang, X.-Y. Bao, H. Kim, Y. Lo, D. Wang, *J. Nanosci. Nanotechnol.* **2010**, *10*, 1–20.
- [5] a) E. Stern, J. F. Klemic, D. A. Routenberg, P. N. Wyrembak, D. B. Turner-Evans, A. D. Hamilton, D. A. LaVan, T. M. Fahmy, M. A. Reed, *Nature* **2007**, *445*, 519–522; b) F. Patolsky, G. Zheng, C. M. Lieber, *Anal. Chem.* **2006**, *78*, 4260–4269.
- [6] a) M. Kuno, *Phys. Chem. Chem. Phys.* **2008**, *10*, 620–639; b) L. Cademartiri, G. A. Ozin, *Adv. Mater.* **2009**, *21*, 1013–1020.
- [7] a) D. Xu, D. Chen, Y. Xu, X. Shi, G. Guo, L. Cui, Y. Tang, *Pure Appl. Chem.* **2000**, *72*, 127–135; b) H. Niu, L. Zhang, M. Y. Gao, Y. M. Chen, *Langmuir* **2005**, *21*, 4205–4210; c) M. C. Kum, B. Y. Yoo, Y. W. Rheem, K. N. Bozhilov, W. Chen, A. Mulchandani, N. V. Myung, *Nanotechnology* **2008**, *19*, 325711; d) H. W. Liang, S. Liu, Q.-S. Wu, S.-H. Yu, *Inorg. Chem.* **2009**, *48*, 4927–4933; e) H.-W. Liang, S. Liu, S.-H. Yu, *Adv. Mater.* **2010**, *22*, 3925–3937.
- [8] a) S. Neretina, R. A. Hughes, J. F. Britten, N. V. Sochinskii, J. S. Preston, P. Mascher, *Nanotechnology* **2007**, *18*, 275301; b) W. Park, H. S. Kim, S. Y. Jang, J. Park, S. Y. Bae, M. Jung, H. Lee, J. Kim, *J. Mater. Chem.* **2008**, *18*, 875–880; c) X. B. Cao, X. M. Lan, Y. Guo, C. Zhao, *Cryst. Growth Des.* **2008**, *8*, 575–580; d) M. I. B. Utama, Z. Peng, R. Chen, B. Peng, X. Xu, Y. Dong, L. M. Wong, S. Wang, H. Sun, Q. Xiong, *Nano Lett.* **2011**, *11*, 3051–3057.
- [9] a) F. D. Wang, A. G. Dong, J. W. Sun, R. Tang, H. Yu, W. E. Buhro, *Inorg. Chem.* **2006**, *45*, 7511–7521; b) J. W. Sun, W. E. Buhro, L.-W. Wang, J. Schrier, *Nano Lett.* **2008**, *8*, 2913–2919; c) M. Kuno, O. Ahmad, V. Protasenko, D. Bacinello, T. H. Kosel, *Chem. Mater.* **2006**, *18*, 5722–5732; d) J. Puthusseri, T. H. Kosel, M. Kuno, *Small* **2009**, *5*, 1112–1116.
- [10] a) Y. D. Li, H. W. Liao, Y. Ding, Y. T. Qian, L. Yang, G. E. Zhou, *Chem. Mater.* **1998**, *10*, 2301–2303; b) Q. Yang, K. B. Tang, C. R. Wang, Y. T. Qian, S. Y. Zhang, *J. Phys. Chem. B* **2002**, *106*, 9227–9230; c) H. Gong, X. P. Hao, C. Gao, Y. Z. Wu, J. Du, X. G. Xu, M. H. Jiang, *Nanotechnology* **2008**, *19*, 445603.
- [11] a) H. Zhang, D. Wang, H. Mohwald, *Angew. Chem., Int. Ed.* **2006**, *45*, 762–765; b) H. Zhang, D. Wang, B. Yang, H. Mohwald, *J. Am. Chem. Soc.* **2006**, *128*, 10171–10180; c) H. J. Niu, M. Y. Gao, *Angew. Chem., Int. Ed.* **2006**, *45*, 6462–6466; d) P. V. Nair, K. G. Thomas, *J. Phys. Chem. Lett.* **2010**, *1*, 2094–2098.
- [12] a) Z. Y. Tang, N. A. Kotov, M. Giersig, *Science* **2002**, *297*, 237–240; b) K. S. Cho, D. V. Talapin, W. Gaschler, C. B. Murray, *J. Am. Chem. Soc.* **2005**, *127*, 7140–7147; c) N. Pradhan, H. Xu, X. Peng, *Nano Lett.* **2006**, *6*, 720–724; d) Z. Zhang, Z. Tang, N. A. Kotov, S. C. Glotzer, *Nano Lett.* **2007**, *7*, 1670–1675; e) K. T. Yong, Y. Sahoo, H. Zeng, M. T. Swihart, J. R. Minter, P. N. Prasad, *Chem. Mater.* **2007**, *19*, 4108–4110; f) F. Jiang, Y. C. Li, M. F. Ye, L. Z. Fan, Y. Q. Ding, Y. F. Li, *Chem. Mater.* **2010**, *19*, 4108–4110; g) X. P. Jin, M. Kruszynska, J. Parisi, J. K. Olesiak, *Nano Res.* **2011**, *4*, 824–835; h) T. Wang, Z. G. Jin, Y. Shi, W. Li, J. Yang, *Cryst. Growth Des.* **2009**, *9*, 5077–5082.
- [13] Q. Zhang, S. J. Liu, S. H. Yu, *J. Mater. Chem.* **2009**, *19*, 191–207.
- [14] a) L. J. Lauhon, Mark S. Gudiksen, C. M. Lieber, *Philos. Trans. R. Soc. London A* **2004**, *362*, 1247–1260; b) J. Hu, Y. Bando, D. Golberg, *J. Mater. Chem.* **2009**, *19*, 330–343; c) J. Schrier, D. O. Demchenko, L.-W. Wang, *Nano Lett.* **2007**, *7*, 2377–2382; d) H. L. Wang, M. Upmanyu, C. V. Ciobanu, *Nano Lett.* **2008**, *8*, 4305–4311; e) T. Sadowski, R. Ramprasad, *J. Phys. Chem. C* **2010**, *114*, 1773–1781.

- [15] a) L. J. Lauhon, M. S. Gudiksen, D. Wang, C. M. Lieber, *Nature* **2002**, *420*, 57–61; b) Y. Wang, Z. Y. Tang, X. R. Liang, L. M. Liz-Marzán, N. A. Kotov, *Nano Lett.* **2004**, *4*, 225–231; c) D. V. Talapin, H. Yu, E. V. Shevchenko, A. Lobo, C. B. Murray, *J. Phys. Chem. C* **2007**, *111*, 14049–14054; d) J. A. Goebel, R. W. Black, J. Puthussery, J. Giblin, T. H. Kosel, M. Kuno, *J. Am. Chem. Soc.* **2008**, *130*, 14822–14831; e) T. Mokari, S. E. Habas, M. J. Zhang, P. D. Yang, *Angew. Chem., Int. Ed.* **2008**, *120*, 5687–5690; f) Z. Li, X. D. Ma, Q. Sun, Z. Wang, J. Liu, Z. H. Zhu, S. Z. Qiao, S. C. Smith, G. Q. Lu, A. Mews, *Eur. J. Inorg. Chem.* **2010**, 4325–4331.
- [16] a) D. J. Milliron, S. M. Hughes, Y. Cui, L. Manna, J. Li, L.W. Wang, A. P. Alivisatos, *Nature* **2004**, *430*, 190–195; b) F. Shieh, A. E. Saunders, B. A. Korgel, *J. Phys. Chem. B* **2005**, *109*, 8538–8542; c) P. Reiss, M. Protière, L. Li, *Small* **2009**, *5*, 154–168; d) M. Shim, H. McDaniel, *Curr. Opin. Solid State Mater. Sci.* **2010**, *14*, 83–94.
- [17] a) W. W. Yu, Y. A. Wang, X. G. Peng, *Chem. Mater.* **2003**, *15*, 4300–4308; b) Y. C. Li, X. H. Li, C. H. Yang, Y. F. Li, *J. Phys. Chem. B* **2004**, *108*, 16002–16011; c) J. W. Cho, H. S. Kim, Y. J. Kim, S. Y. Jang, J. Park, *Chem. Mater.* **2008**, *20*, 5600–5609.
- [18] a) Z. A. Peng, X. G. Peng, *J. Am. Chem. Soc.* **2002**, *124*, 3343–3353; b) C. C. Kang, C. W. Lai, H. C. Peng, J. J. Shyue, P. T. Chou, *Small* **2007**, *3*, 1882–1885; c) L. F. Xi, W. Xiu, W. Tan, C. Boothroyd, Y. M. Lam, *Chem. Mater.* **2008**, *20*, 5444–5452; d) L. F. Xi, Y. M. Lam, *Chem. Mater.* **2009**, *21*, 3710–3718.
- [19] H. T. Liu, J. S. Owen, A. P. Alivisatos, *J. Am. Chem. Soc.* **2007**, *129*, 305–312.
- [20] Wang equation: $E_{\text{gn}} = [E_{\text{gb}}^2 + \frac{2E_{\text{gb}}h^2}{m^*D^2}]^{1/2}$, where E_{gn} and E_{gb} are the band gap of the semiconductor nanoparticle and its bulk material, respectively, D is the particle size, and m^* is the average of the reciprocals of the effective mass of an electron (m_e^*) and hole (m_h^*). For CdTe, m_e^* and m_h^* are reported to $0.11m_0$ and $0.35m_0$. Details regarding this equation and the related parameters can be found, respectively in the references: a) Y. Wang, A. Suna, W. Mahler, R. Kasowski, *J. Chem. Phys.* **1987**, *87*, 7315; b) S. Kasap, P. Capper, *Springer Handbook of Electronic and Photonic Materials*, Springer, Berlin **2007**.
- [21] I. V. Markov, *Crystal Growth for Beginners: Fundamentals of Nucleation, Crystal Growth, and Epitaxy*, World Scientific, Singapore **1995**.
- [22] a) K. Yu, B. Zaman, S. Romanova, D. Wang, J. A. Ripmeester, *Small* **2005**, *1*, 332–338; b) P. T. K. Chin, C. D. M. Donegá, S. S. V. Bavel, S. C. J. Meskers, N. A. J. M. Sommerdijk, R. A. J. Janssen, *J. Am. Chem. Soc.* **2007**, *129*, 14880–14886.
- [23] Equation (1): $\Delta V_{\text{total}} = \pi L[(R + nd)^2 - R^2]$, Equation (2): $\Delta V_n = \pi L[2Rd + (2n - 1)d^2]$, where ΔV_{total} and ΔV are the volume of the shell composed of n monolayers (nm^3) and the volume of one specified shell monolayer (nm^3), respectively, R (nm) and L (nm) are the diameter and length of the core nanowire respectively, and d (nm) is the average thickness of one shell monolayer.